Polymer Journal (2023) 55:885–895
https://doi.org/10.1038/s41428-023-00787-4

ORIGINAL ARTICLE

Water-soluble guanidinylated chitosan: a candidate material for protein delivery systems

Hironori Izawa[1,2,3] · Ayaka Yagi[4] · Ryo Umemoto[4] · Shinsuke Ifuku[2,3]

Received: 26 January 2023 / Revised: 16 March 2023 / Accepted: 3 April 2023 / Published online: 10 May 2023

Abstract

Here, we introduce water-soluble guanidinylated chitosan (WGCS) as a candidate material for protein delivery systems to enhance the cellular internalization of protein/peptide drugs. A WGCS composed of 48.2% guanidinylated chitosan, 20.6% chitosan, and 31.2% chitin units was prepared with a low-molecular-weight chitosan (CS) lactate via a guanidinylation reaction with 1-amidinopyrazole hydrochloride. The M_n of WGCS was estimated by gel permeation chromatography analysis to be 7.6×10^3 ($M_w/M_n = 1.5$). The higher chitin content in WGCS than in common CS (<20%) is an important factor in achieving water solubility. WGCS showed ca. 2.5-fold higher internalization into HeLa cells than CS does. This clearly indicated that guanidinylation enhances internalization. In addition, endocytic pathways were suggested as a mechanism underlying internalization. Moreover, WGCS significantly enhanced the internalization of bovine serum albumin (BSA) in transport medium at pH 7.4 containing BSA: the internalized amount of BSA in the presence of WGCS was ca. 2-fold higher than in the presence of CS. This higher internalization was caused by efficient binding between WGCS and BSA via electrostatic interactions owing to the guanidino groups. Indeed, the affinity of the binding sites of WGCS is more than 10-fold higher than that of the binding sites of CS.

Introduction

Although advances in medicines and medical technologies have enabled the treatment of numerous diseases, many intractable diseases still have no established treatments [1]. Protein/peptide drugs have attracted a great deal of attention as possible therapeutic treatments for such diseases. Progress in biotechnology has enabled the production of various protein/peptide drugs for therapeutic uses. However, the poor membrane permeability of these drugs due to their high molecular weight (>500 Da) limits their cellular internalization [2]. Improving permeability remains a great challenge despite considerable efforts to develop novel formulations to overcome those problems [3–8]. We believe that a breakthrough toward this end will rely on the development of highly permeable materials that are readily available.

Chitosan (CS) is an amino polysaccharide produced by the deacetylation of chitin [9–11]. CS is often used for protein delivery systems to overcome the abovementioned problem because CS can conjugate to protein/peptide drugs via electrostatic interactions and can promote the membrane permeation of the complex because of its amino groups [3]. In general, the characteristic functions of CSs rely on amino groups. In addition, the higher reactivity of amino groups enables the facile modification of CSs to develop functionalized CS derivatives. On the other hand, common CSs are soluble only in acidic media because the higher protonation of an amino group at acidic pH than at neutral pH contributes to the breaking of hydrogen bonds [12]; that is, common CSs are insoluble at neutral pH. This lack of

Supplementary information The online version contains supplementary material available at https://doi.org/10.1038/s41428-023-00787-4.

✉ Hironori Izawa
h-izawa@cc.miyazaki-u.ac.jp

[1] Faculty of Engineering, University of Miyazaki, 1-1 Gakuen Kibanadai-Nishi, Miyazaki 889-2192, Japan

[2] Department of Chemistry and Biotechnology, Faculty of Engineering, Tottori University, 4-101 Koyama-Minami, Tottori 680-8550, Japan

[3] Center for Research on Green Sustainable Chemistry, Tottori University, Tottori 680-8550, Japan

[4] Graduate School of Sustainability Science, Tottori University, 4-101 Koyama-Minami, Tottori 680-8550, Japan

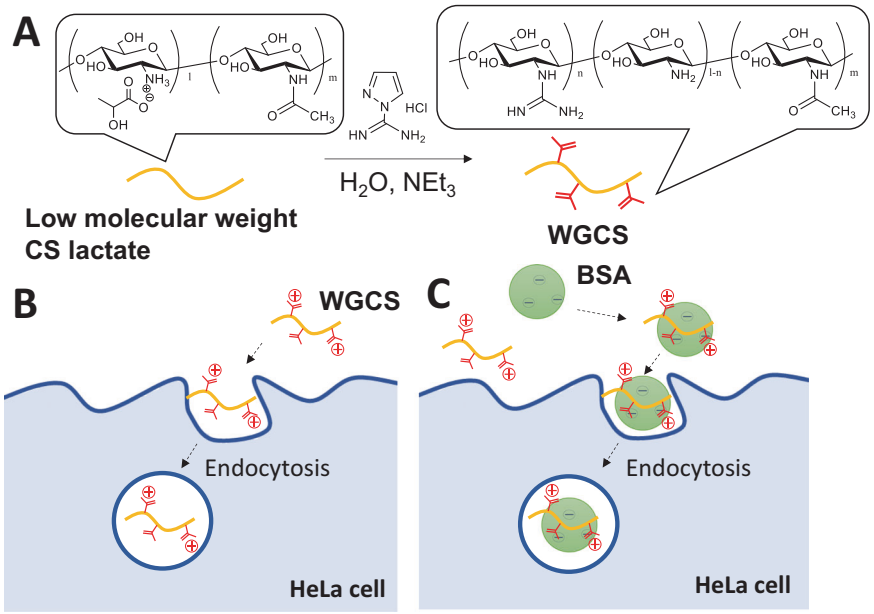

Fig. 1 Illustration of this study. Preparation of WGCS (**A**), internalization of WGCS (**B**), and BSA in the presence of WGCS (**C**)

solubility at biological pH hinders the application of CSs to drug delivery systems (DDSs) [13]. Therefore, water-soluble CSs are developed by controlling the molecular weight [14, 15] and/or the degree of deacetylation [16–18] or by chemical modification [19, 20]. In addition, the conjugation of CSs and CS derivatives with other materials, such as liposomes [21], inorganic materials [22], and polymers [23], via electrostatic interactions can also enable the use of CSs and CS derivatives to develop novel DDSs.

We previously reported a simple method for producing guanidinylated chitosan (GCS) with 1-amidinopyrazole hydrochloride (AP) [24, 25]. GCS enhances electrostatic interactions with protein/peptide drugs under biological conditions because the guanidino group has lower acidity (pKa: 12.5 in protonated form) than the amino group (pKa: 6.5 in protonated form) [26]. GCS should also enhance the membrane permeability of drugs, similar to with the behavior of arginine-rich cell-penetrating peptides [27–30]. However, the performance of GCS in improving membrane permeability has not yet been investigated. In addition, although other researchers have synthesized GCSs for antibacterial, tissue engineering, and gene delivery uses, a water-soluble GCS (WGCS) has not been previously reported [31–34]. We believe that a WGCS that is useable at biological pH is an ideal candidate material for taking full advantage of the performance of guanidino groups to develop various DDSs, including protein delivery systems.

Here, we show the preparation of WGCS and its cellular internalization (Fig. 1). WGCS is prepared by the guanidinylation of low-molecular-weight CS lactate ($M_n = 5.6 \times 10^3$) with AP. This CS lactate displays water solubility even at alkaline pH because of its relatively low molecular weight. Therefore, we expected that WGCS made with CS lactate to show solubility at approximately neutral pH. After we evaluated the cytotoxicity of WGCS, we investigated its cellular internalization into HeLa cells. In addition, we examined the cellular internalization of bovine serum albumin (BSA) as a model protein drug incorporated with WGCS.

Experimental procedures

Materials

CS lactate was purchased from Koyo Chemical Co., Ltd. (Tottori, Japan). The value of M_n estimated by gel permeation chromatography (GPC) analysis with pullulan standards was 5.6×10^3 ($M_W/M_n = 2.4$); the degree of deacetylation estimated by elemental analysis was 68.8%. AP and 1-(3-dimethylaminopropyl)-3-ethylcarbodiimide hydrochloride (EDC) were purchased from Tokyo Chemical Industry Co., Ltd. (Tokyo, Japan). Fluorescein isothiocyanate-dextran (FD4, average molecular weight 3000–5000), Dulbecco's modified Eagle medium, high glucose (DMEM), and bovine serum albumin–fluorescein isothiocyanate conjugate (F-BSA) were purchased from Sigma–Aldrich (St. Louis, MO, USA). Triethylamine, *N*-hydroxysuccinimide (NHS), Cellstain Hoechst 33342 solution, and octaarginine (R8) were purchased from Fujifilm-Wako Co., Ltd. (Tokyo, Japan). A HeLa cell line (CH3 BioSystems, Amherst, NY, USA) was purchased from Funakoshi Co., Ltd. (Tokyo, Japan). Antibiotic–antimycotic solution (100×), MEM nonessential amino acids solution (10×), fetal bovine serum (qualified, US) (FBS), Hank's balanced salt solution (HBSS) (10×), phosphate-buffered saline (pH 7.4, 10×) (PBS), Trypan blue, and LysoTracker Green were purchased from Thermo Fisher Scientific (Waltham,

MA, USA). An MTT (3-(4,5-dimethylthiazol-2-yl)-2,5-diphenyltetrazolium bromide) cell counting kit (product code: 23506-80) and HEPES (4-(2-hydroxyethyl)-1-piperazineethanesulfonic acid) were purchased from Nacalai Tesque, Inc. (Kyoto, Japan). Other reagents were obtained at commercial grade and used without further purification.

Measurements

^{1}H nuclear magnetic resonance (NMR) spectra were acquired on a JNM-ECP500 (JEOL, Tokyo, Japan). Elemental analysis data were recorded on a Perkin Elmer 2400 II CHNS/O (Perkin Elmer, Waltham, MA, USA). M_n and M_w/M_n of CS lactate and WGCS were measured by GPC at 40 °C in acetate buffer solution eluent: Asahipak GS-220 HQ, Asahipak GS-320 HQ, Asahipak GS-520 HQ, and Asahipak GS-2G 7B (Shodex, Japan); an L-2130 pump, and an L-2490 RI detector (Hitachi, Japan). The flow rate was 0.5 mL/min. Interactions between WGCS and F-BSA/FD4 were analyzed with the BLItz system (ForteBio, Fremont, CA, USA). Absorbance values for the MTT assay were recorded on a Multiskan GO (Thermo Fischer Scientific). Fluorescence spectra were recorded on an RF-6000 (Shimadzu, Kyoto, Japan). Confocal laser scanning microscopy (CLSM) images were recorded by a Fluoview FV10i (Olympus, Tokyo, Japan) with an excitation light at 405 nm (Hoechst 33342) or 473 nm (LysoTracker Green, R-CS, R-WGCS, and F-BSA) and a blue filter (Hoechst 33342), green filter (LysoTracker and F-BSA), or red filter (R-CS and R-WGCS). Dynamic light scattering (DLS) was performed with an ELSZ-1000 zeta potential and particle size analyzer (Otsuka Electronics Co., Ltd., Japan).

Synthesis of WGCS

CS lactate (1.00 g, chitosan unit: 2.91 mmol) was dissolved in distilled water (2.2 mL). AP (1.75 g, 11.9 mmol) was added to the CS lactate solution, and the mixture was stirred for 10 min. Triethylamine (1.45 g, 14.3 mmol) was added, and the mixture was vigorously stirred for 7 days at room temperature. The reaction mixture was subsequently poured into a large volume of isopropanol, and the precipitated product was collected by filtration and then washed with methanol. The crude product was purified by dialysis with a Visking tube (molecular weight cutoff: 3500) in a large volume of water. The yield of the lyophilized product was 0.621 g. ^{1}H NMR (500 MHz, CD_3COOD-D_2O, 80 °C) $\delta = 2.00$ ($C\underline{H}_3CO$- and $\underline{H}CD_2COOD$ in CD_3COOD), 2.13 (CS and GCS units, H-2), 3.45–3.85 (the other sugar protons, CS and GCS units), 4.53 (CS and GCS units, H-1), 4.81 (*N*-acetylglucosamine unit, H-1). IR (cm^{-1}, neat) 3320, 2896, 2865, 1710, 1640, 1582, 1549, 1376, 1317, 1030. Elemental analysis C 39.07 H 6.63 N 12.60.

Filtration experiment of WGCS aqueous solution

WGCS (30.2 mg) was added to 10 mL of water and stirred for 1 h at room temperature. The WGCS solution was passed through a syringe filter (Millipore Millex-GV; 0.45 μm). Additional water (5 mL) was passed through to push out the WGCS solution remaining in the syringe filter. The passed WGCS solution was lyophilized. The weight of the lyophilized material was 27.4 mg.

Preparation of culture or transport medium

Culture medium [35]: Culture medium was prepared by mixing DMEM (450 mL), antibiotic–antimycotic solution (2.5 mL), MEM nonessential amino acids solution (5 mL), and FBS (50 mL).

Transport medium [35]: Glucose (2.5 g), HEPES (2.25 g), $NaHCO_3$ (0.35 g), HBSS (100 mL), and an appropriate amount of WGCS/CS lactate solution (cytotoxicity assay) or 2.5 mg/mL WGCS/CS with the rhodamine group (R-WGCS/R-CS) solution prepared in 0.1 M acetic acid (100 mL; cellular internalization experiment) were mixed in ultrapure water (0.7 L), and the total volume and pH of the solution were adjusted to 1.0 L and 7.4, respectively. The transport medium was filtered by a syringe filter (Millipore Millex-GV; 0.45 μm) for sterilization.

Cytotoxicity assay

A HeLa cell suspension (100 μL; 5.0×10^4 cells/mL cells diluted by the culture medium) was seeded on 96-well culture plates (FALCON®, Corning, Corning, NY, USA) and cultured for 24 h (37 °C, 5% CO_2). After incubation, the culture medium was removed, and the cells were washed twice with HBSS. Transport medium (pH 7.4) containing WGCS or CS lactate was added, followed by incubation for 24 h (37 °C, 5% CO_2). MTT solution (10 μL) was added, followed by further incubation for 4 h (37 °C, 5% CO_2). Formazan solubilization solution (100 μL) was added, followed by incubation at 37 °C for 4 h. The absorbance at 570 nm (reference: 650 nm) was recorded by a microplate reader. Cell viability was determined by the following equation:

$$\text{Cell viability}(\%) = \frac{\text{Absorbance of sample solution}}{\text{Absorbance of blank solution}} \times 100. \quad (1)$$

Cellular internalization of WGCS

HeLa cell suspension (2.2 mL; 6.0×10^4 cells/mL cells diluted by the culture medium) was seeded on a cell culture dish with a glass bottom (dish diameter: 35 mm, glass

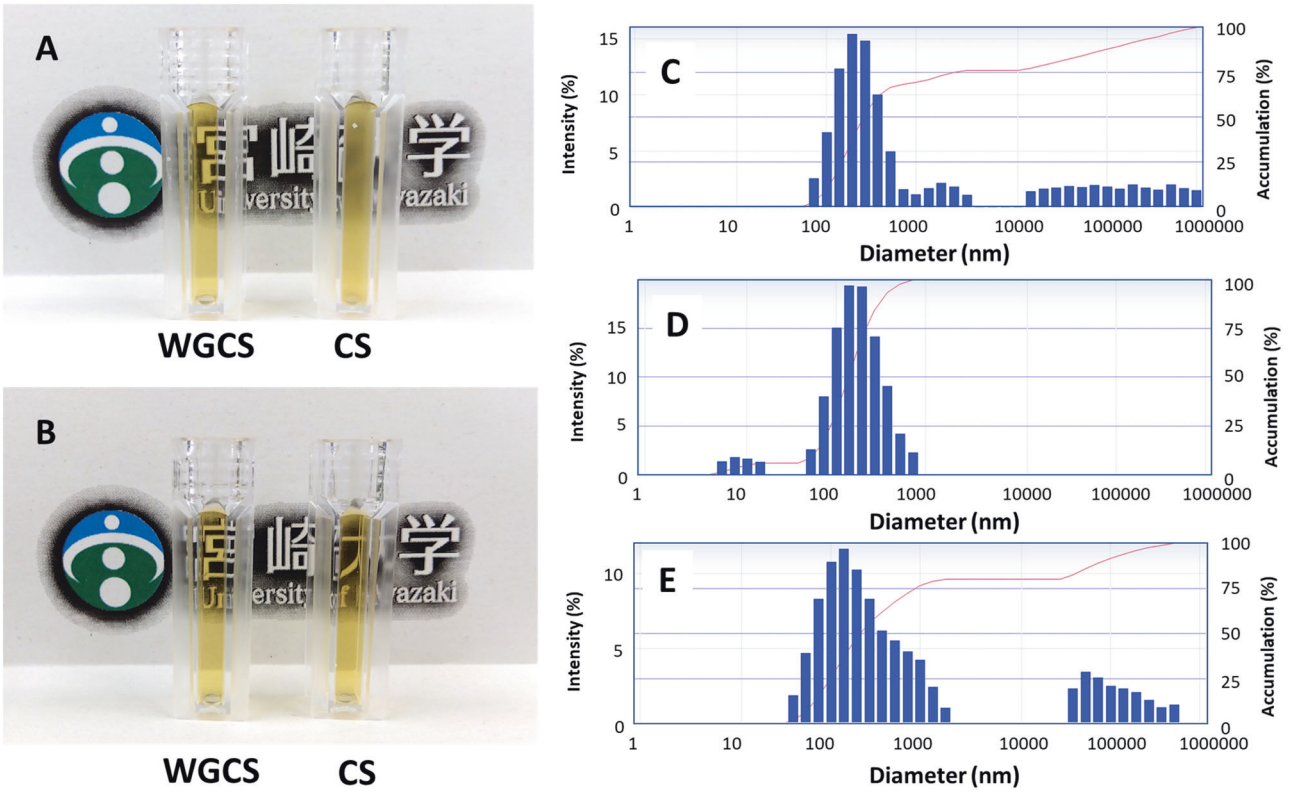

Fig. 2 Photographic images of 3 mg/mL WGCS and CS solutions (water; **A**, 0.1 M acetic acid solution; **B**) and their DLS diagrams (WGCS in water; **C**, WGCS in 0.1 M acetic acid solution; **D**, CS in 0.1 M acetic acid solution; **E**)

diameter: 14 mm) and cultured for 72 h (37 °C, 5% CO_2). After incubation, the culture medium was removed, and the cells were washed twice with HBSS. Transport medium containing 0.25 mg/mL R-WGCS/R-CS and 10 μg/mL Hoechst 33342 or 50 nM LysoTracker Green was added, and the mixture was incubated for 4 h (37 °C, 5% CO_2). The transport medium was removed and washed twice with PBS. PBS (3 mL) was added, and the adhered cells were observed by CLSM analysis. After observation, the cells were detached with trypsin. The number of detached cells was counted by a hemocytometer with an optical microscope. The cells were crushed by sonication, and the fluorescence spectra with excitation at 550 nm for the rhodamine group on R-WGCS/R-CS were recorded.

Cellular internalization of BSA or FD4 in the presence of WGCS

HeLa cell solution (2.2 mL; 6.0×10^4 cells/mL cells diluted by the culture medium) was seeded on a cell culture dish with a glass bottom (dish diameter: 35 mm, glass diameter: 14 mm) and cultured for 72 h (37 °C, 5% CO_2). After incubation, the culture medium was removed, and the cells were washed twice with HBSS. Transport medium containing 0.25 mg/mL R-WGCS/R-CS and 2.5 mg/mL FD4/F-BSA was added, and the mixture was incubated for 4 h (37 °C, 5% CO_2). The transport medium was removed and washed twice with PBS. PBS (3 mL) was added, and the adhered cells were observed by CLSM analysis. After observation, the cells were detached with trypsin. The number of detached cells was counted by a hemocytometer with an optical microscope. The cells were crushed by sonication, and fluorescence spectra with excitation at 490 nm for the fluorescein group in FD4/F-BSA were recorded.

Biolayer interferometry analysis

AR2 fiber sensors with carboxy groups were dipped into 10 mM HEPES buffer (pH 7.4) for 30 s, then into 1 mg/mL EDC-NHS solution (HEPES buffer, pH 7.4) for 300 s for activation, followed by dipping into 0.5 mg/mL WGCS or CS solution (HEPES buffer, pH 7.4). The sensors were then dipped into 10 mM HEPES buffer for 300 s to obtain a baseline, and the GCS- and CS-immobilized sensors were then dipped into 100 μg/mL F-BSA or FD4 for 300 s to observe association behavior. The sensors were then dipped into 10 mM HEPES buffer for 300 s to observe dissociation behavior.

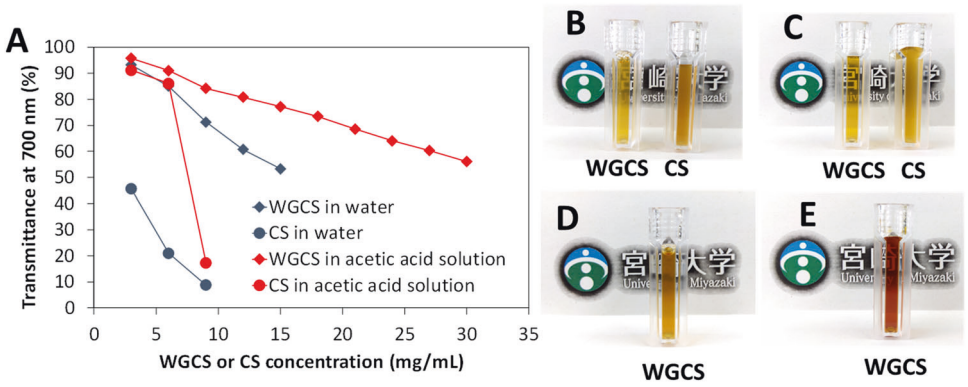

Fig. 3 Transmittances of WGCS and CS solutions prepared in water or 0.1 M acetic acid at 700 nm (**A**). Photographic images of 9 mg/mL WGCS and CS solutions (water; **B**, 0.1 M acetic acid; **C**), 15 mg/mL WGCS in water (**D**), and 30 mg/mL WGCS in 0.1 M acetic acid (**E**)

Results and discussion

Synthesis of WGCS

CS lactate was guanidinylated in accordance with a previous report (Fig. 1A) [24]. The production of WGCS was confirmed by ^{1}H NMR and IR analyses (Figs. S1 and S2). The degree of guanidinylation (GCS unit (mol)/total unit (mol) × 100) estimated from elemental analysis was 48.2%; i.e., WGCS was composed of 48.2% GCS, 20.6% CS, and 31.2% chitin units. The M_n estimated by GPC analysis with pullulan standards was 7.6×10^3 ($M_w/M_n = 1.5$), which is higher than that of the CS lactate. This is due to removal of the oligosaccharide fraction in the product through dialysis with a Visking tube (molecular weight cutoff 3500) (Fig. S3). Note that the WGCS was not in salt form because acids such as lactic acid and HCl were removed by dialysis.

Solubility of WGCS

The solubility of WGCS was investigated. We prepared CS as a sample for comparison with the no-guanidino group by dialysis of the CS lactate. Both WGCS and CS were soluble in 0.1 M acetic acid solution, similar to common CSs (Fig. 2B). On the other hand, in water, WGCS dissolved completely, but CS had a visible water-insoluble fraction (Fig. 2A). Figure 2C–E show DLS diagrams of the WGCS and CS solutions. In the case of WGCS in water, light scattering due to invisible microscopic aggregates above 10 µm was observed, indicating the presence of a water-insoluble fraction. In addition, the presence of microscopic aggregates was also observed in the CS solution prepared with 0.1 M acetic acid solution. However, light scattering above 10 µm was not observed in the WGCS solution prepared with 0.1 M acetic acid solution. Figure 3A shows the transmittances of the WGCS and CS solutions at 700 nm. In the case of CS in water, the transmittance rapidly decreased at 9 mg/mL due to the pH change caused by CS. This decrease in transmittance was not observed in 9 mg/mL WGCS in water (Fig. 3B), indicating that the guanidino group in WGCS contributed to the improvement of solubility. Although we confirmed that WGCS is soluble in water, the transmittances of WGCS in water were lower than those in acetic acid. WGCS solutions prepared with water gradually became more turbid as the WGCS concentration increased due to the presence of microscopic aggregates detected in the DLS analysis (Fig. 3D). In contrast, WGCS solutions prepared with 0.1 M acetic acid solution were transparent even at 30 mg/mL (Fig. 3E). This observation also indicates the presence of a water-insoluble fraction in WGCS. Therefore, we additionally checked for the presence of microscopic aggregates in the WGCS solution prepared with water by passing the solution through a syringe filter with 0.45-µm pores; i.e., we defined a removed fraction as an insoluble part. The 3 mg/mL WGCS solution prepared with water passed through the syringe filter. The weight of the passed WGCS was 90.7%, indicating that 9.3% of WGCS was water insoluble. Note that 3 mg/mL WGCS and the low-molecular-weight CS were not precipitated out after dissolution into acetic acid solution and subsequent neutralization by adding NaOH solution.

We investigated the effect of the degree of acetylation on the water solubility of GCS because WGCS has a higher chitin content (degree of acetylation = 31.2%) than a common CS (<20%), as described above. GCS with a lower chitin content, composed of 56.4% GCS, 32.4% CS, and 11.2% chitin units, was prepared from a CS lactate with a degree of acetylation of 11.2% ($M_n = 6.2 \times 10^3$, $M_w/M_n = 1.6$, Fig. S4). Interestingly, the solubility of the GCS with a lower chitin content was different from that of the WGCS. The GCS with a lower chitin content was insoluble in water but soluble in 0.1 M acetic acid solution (Fig. S5). However, 3 mg/mL GCS with a lower chitin content prepared in 0.1 M acetic acid was turbid due to scattering caused by microscopic aggregates. Indeed, the transmittance of the solution at 700 nm was 63.7%, which was lower than that of WGCS. This result strongly suggests that the guanidino group in GCS with a lower chitin content reduced its solubility in both water and acetic acid solutions. Thus, the

degree of acetylation is an important factor in controlling the solubility of GCS. Similar water solubility enhancement due to an increased degree of acetylation was observed in water-soluble CSs with a 50% degree of acetylation, where water solubility was enhanced by virtue of lower crystallinity, highly increased hydrophilicity, and electrostatic repulsion [16, 18].

Cytotoxicity of WGCS

The cytotoxicity of WGCS to a HeLa cell line was investigated using the MTT assay. Figure 4 shows the cell viabilities of HeLa cells after incubation in transport medium containing 0.25–4.0 mg/mL CS lactate or WGCS for 24 h (37 °C, 5% CO_2). The cell viabilities for 0.25 mg/mL and 0.50 mg/mL CS lactate were 93.9 ± 5.5% and 94.8 ± 4.7%, respectively. Viability gradually decreased as the CS lactate level increased above 1.0 mg/mL. In the case of WGCS, cell viability at 0.25 mg/mL was 92.2 ± 7.0%, which was comparable to that of CS lactate. Viability gradually decreased as WGCS increased. Notably, the cell viabilities of WGCS were significantly lower than those of CS lactate above 1.0 mg/mL. This suggested that larger amounts of WGCS molecules were taken up into HeLa cells than CS molecules by virtue of the guanidino groups; however, this increased cell death. In addition, this cytotoxicity assay revealed that we can perform cellular internalization experiments with transport media containing 0.25 mg/mL WGCS or CS lactate.

Cellular internalization of WGCS

To evaluate the membrane permeability of WGCS (Fig. 1B), HeLa cells were precultured with culture medium and incubated in transport medium (pH 7.4) containing Hoechst 33342 for fluorescence imaging of nuclei and R-WGCS or R-CS containing rhodamine B (Scheme S1 and Fig. S6) for 4 h (37 °C, 5% CO_2). Figure 5A shows CLSM images of the HeLa cells after incubation. In both cases, regions of red fluorescence owing to R-WGCS and R-CS were observed throughout the cytosol. The red fluorescence regions were stronger in R-WGCS than in R-CS, suggesting that a larger number of R-WGCS molecules were taken up by HeLa cells. In addition, there were areas of strong red fluorescence, suggesting the accumulation of R-WGCS molecules in some organelles. The internalized amounts of R-WGCS and R-CS were determined by the fluorescence spectra of HeLa cells that were peeled off after incubation and then crushed by sonication (Fig. 5C). The internalized amounts were normalized to the number of cells (Fig. 5D). The internalized amount of R-WGCS was ca. 2.5-fold higher than that of R-CS, indicating that the guanidino group in WGCS contributed to the enhancement of membrane permeability.

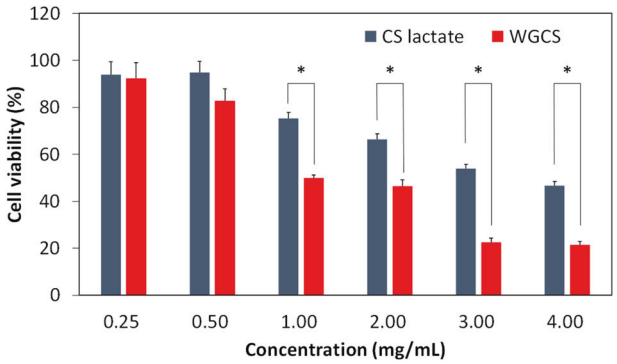

Fig. 4 Cell viabilities of CS lactate and WGCS toward a HeLa cell line. Error bars reflect the standard deviations ($n = 3$, $^*p < 0.05$)

Endocytosis is a major internalization route of arginine-rich CPPs [30]. Therefore, we hypothesized that WGCS is also internalized via endocytic pathways and consequently accumulates in lysosomes. To test this hypothesis, we investigated the colocalization of R-WGCS and LysoTracker Green, which is a marker for lysosomes and acidic vesicles (Fig. 5B). After 4 h of incubation, HeLa cells showed both green fluorescence regions due to LysoTracker Green and red fluorescence regions due to R-WGCS. In the merged images, yellow regions reflecting the colocalization of R-WGCS and LysoTracker Green were observed in the cytosol and some organelles accumulating R-WGCS. This colocalization supports the internalization of R-WGCS via endocytic pathways and the accumulation of R-WGCS in lysosomes [36].

Protein drug internalization in the presence of WGCS

We expected that WGCS molecules would bind to protein drugs via electrostatic interactions and that the complexes would internalize, as in the case of CPPs (Fig. 1C) [28, 37, 38]. Therefore, we investigated the performance of WGCS as an additive to enhance the cellular internalization of bovine serum albumin–fluorescein isothiocyanate conjugate (F-BSA, ca. 66 kDa), which is used as a model protein drug, in the presence of WGCS into HeLa cells. In addition, we investigated the internalization of fluorescein isothiocyanate–dextran (FD4, average molecular weight 3000–5000), a neutral medium-molecular-weight model drug [39]. Fig. 6A shows a CLSM image after incubation in transport medium containing 0.25 mg/mL R-WGCS or R-CS and 2.5 mg/mL F-BSA for 4 h (37 °C, 5% CO_2). In the case of R-WGCS, stronger green fluorescence regions due to F-BSA were observed in HeLa cells. In addition, colocalization of R-WGCS and F-BSA was observed in the merged image. The average F-BSA quantities determined

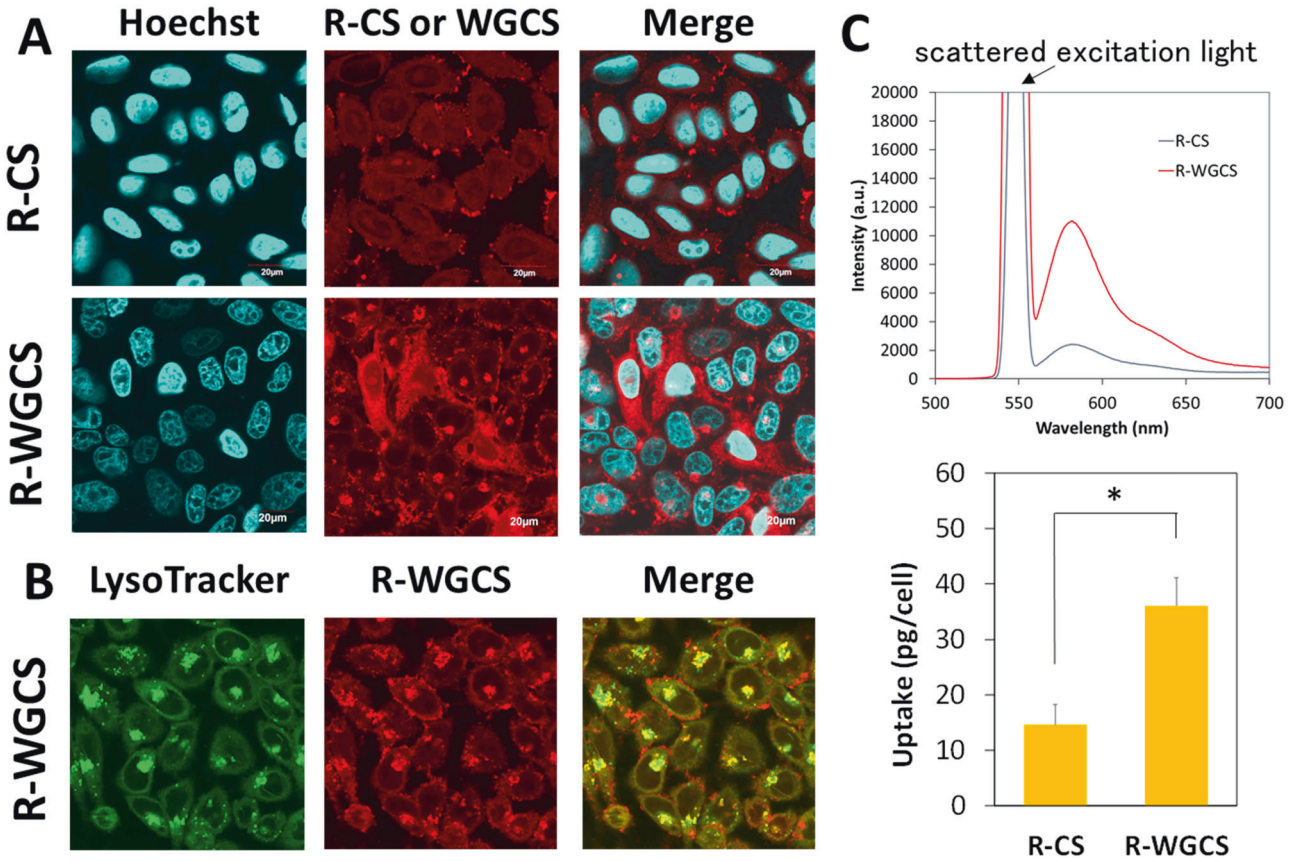

Fig. 5 CLSM images of HeLa cells after incubation in transport medium (pH 7.4) containing 0.25 mg/mL R-CS or R-WGCS and 10 μg/mL Hoechst 33342 for 4 h (37 °C, 5% CO_2) (**A**) and after incubation in transport medium containing 0.25 mg/mL R-WGCS and 50 nM LysoTracker Green for 4 h (37 °C, 5% CO_2) (**B**). Representative fluorescence spectra of R-CS and R-WGCS uptake by HeLa cells (upper) and average internalized amounts (lower) (**C**). Error bars reflect the standard deviations ($n = 3$, $^*p < 0.05$)

from the fluorescence spectra of peeled HeLa cells for R-WGCS or R-CS were 19.5 ± 3.0 and 8.3 ± 2.4 pg/cell, respectively. The internalized amount of F-BSA in the presence of WGCS was ca. 2-fold higher than that in the presence of R-CS. In addition, we investigated the performance of octaarginine (R8), a representative arginine-rich CPP, as an example for comparison [37]. The internalized amount of F-BSA in the presence of R8 was comparable to that in the presence of R-WGCS (19.0 ± 4.1 pg/cell). This result indicates that WGCS is a candidate for the development of a protein delivery system. On the other hand, although WGCS enhanced the internalization of FD4, the effect was comparable to that of the positive controls (CS and R8). We suppose that complex formation via electrostatic interactions between R-WGCS and F-BSA is an important phenomenon for inducing enhanced cellular internalization.

We investigated the interaction between WGCS or CS and F-BSA or FD4 at pH 7.4 by biolayer interferometry analysis with the BLItz system, which allowed us to monitor the change in wavelength shift (Δλ) induced by association (Fig. 7A, B) [40]. The sensorgrams of Δλ were treated in the same way as the well-known Biacore surface plasmon resonance system [41]. In all cases, Δλ values after immobilization of WGCS or CS molecules were approximately 1.7–1.9 nm, indicating that comparable quantities of WGCS and CS molecules were immobilized on the sensors. After dipping in FD4 solution, Δλ values did not show significant increases, indicating that the interaction between WGCS or CS molecules and FD4 is very weak due to a lack of electrostatic interaction. In contrast, the Δλ values for WGCS and CS increased in the case of F-BSA. The increase in Δλ from the baseline after association (ΔΔλ), correlating to the adsorbed quantity of WGCS or CS molecules, was 0.8 nm and 0.2 nm, respectively. This result clearly indicates that the amount of F-BSAs bound to WGCS molecules is higher than that to CS molecules. However, 100 μg/mL F-BSA solution was too high a concentration for this WGCS-BSA system because dissociation behavior (decreasing Δλ) was observed after rapid adsorption behavior (initial rapid Δλ increases at approximately 960 sec) in the association process. Therefore, stepwise associations to evaluate the adsorption of F-BSA onto the WGCS layer in varying F-BSA concentrations were carried

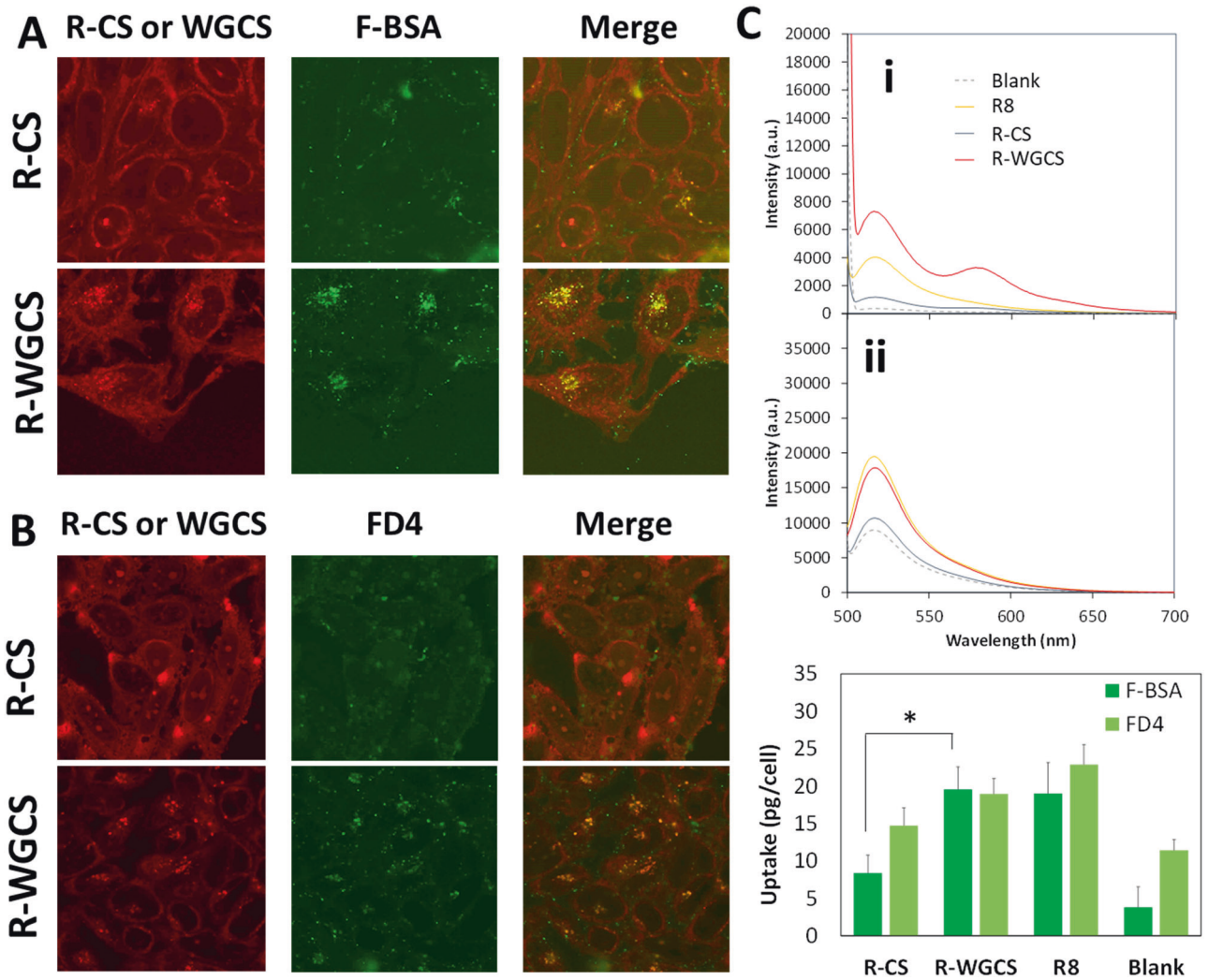

Fig. 6 CLSM images of HeLa cells after incubation in transport medium containing 0.25 mg/mL R-CS or R-WGCS and 2.5 mg/mL F-BSA (**A**) or FD4 (**B**) for 4 h (37 °C, 5% CO_2). Representative fluorescence spectra of F-BSA (i) and FD4 (ii) uptake by HeLa cells in the presence of R-CS, R-WGCS, or R8 (upper) and average internalized amounts (lower) (**C**). Error bars reflect the standard deviations ($n = 3$, $^*p < 0.05$)

out with lower F-BSA concentrations. Figure 7C shows sensorgrams of the stepwise associations with 1–5 μg/mL and 20–100 μg/mL F-BSA solutions for the WGCS and CS layers, respectively. The ΔΔλ values of each F-BSA concentration were subjected to the Langmuir adsorption isotherm as follows [42]:

$$\frac{C_{BSA}}{\Delta\Delta\lambda} = \frac{1}{\alpha q_{max}} + \frac{C_{BSA}}{q_{max}}, \quad (2)$$

where C_{BSA}, α, and q_{max} are the equilibrium concentration of F-BSA, the Langmuir adsorption constant related to the affinity of binding sites, and the maximum adsorption capacity when the adsorbent is fully saturated, respectively. We assumed C_{BSA} values as the initial F-BSA concentrations because large excess amounts of F-BSA are present in the system. Figure 7D shows the Langmuir adsorption isotherms between C_{BSA} and ΔΔλ in the WGCS- or CS-BSA system. In both cases, good linear correlations were observed. The q_{max} and α values estimated from slopes and intercepts between WGCS or CS and F-BSA were 1.37 nm and 0.0449 nM^{-1} or 0.618 nm and 0.00408 nM^{-1}, respectively. Although these values cannot be compared with q_{max} and α values reported in other reports estimated from changes in adsorbed amounts, we can use them for comparison between WGCS and CS. The affinity of the binding sites of WGCS is ca. 11-fold higher than that of CS. This is probably due to salt bridge formation by guanidino groups in WGCS and oxyanions in F-BSA at multiple sites [26]. In addition, the number of binding sites of WGCS for F-BSA was ca. 2-fold higher than that of CS. This is a reasonable result because the WGCS should have higher net positive

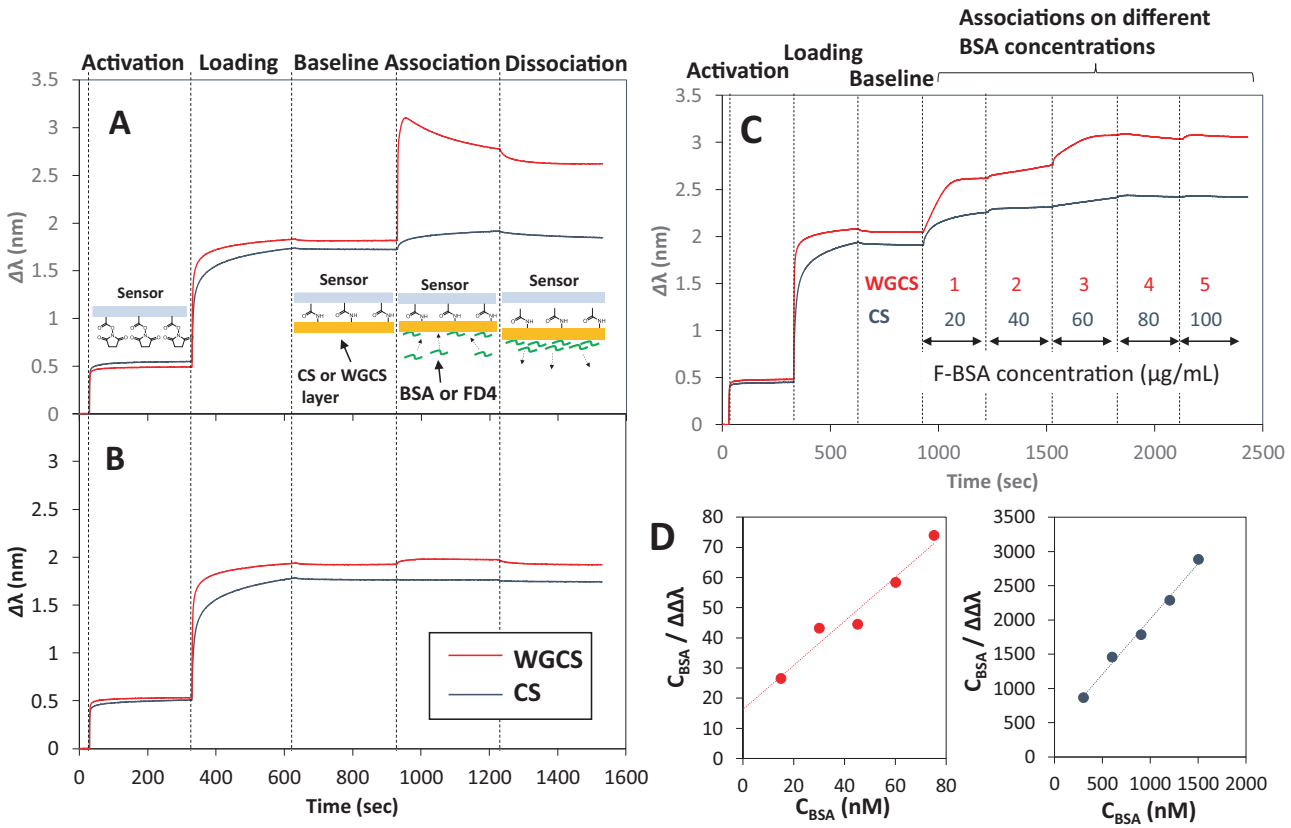

Fig. 7 Biolayer interferometry sensorgrams to evaluate the adsorption of F-BSA (**A**) or FD4 (**B**) onto the WGCS/CS layer. After immobilization of GCS/CS molecules, a fiber sensor was dipped into 100 μg/mL BSA solution (10 mM HEPES buffer, pH 7.4), followed by dipping into 10 mM HEPES buffer for 300 s at room temperature. Biolayer interferometry sensorgram to evaluate adsorption of F-BSA onto the WGCS/CS layer in varying F-BSA concentrations (**C**); a fiber sensor with the WGCS or CS layer was dipped into 1, 2, 3, 4, and 5 μg/mL or 20, 40, 60, 80, and 100 μg/mL F-BSA solutions (10 mM HEPES buffer, pH 7.4), respectively, for 300 s at room temperature. The Langmuir isotherms for the WGCS-BSA (left) and CS-BSA (right) systems (**D**)

charges than the CS at pH 7.4 owing to the presence of guanidino groups. The average q_{max} and α values between WGCS or CS and F-BSA were 1.36 ± 0.10 nm and 0.0813 ± 0.0367 nM^{-1} or 0.625 ± 0.060 nm and 0.00432 ± 0.00088 nM^{-1}, respectively ($n = 3$, $p < 0.05$). This result indicates that the interaction between WGCS and F-BSA was significantly enhanced by the guanidino group.

Conclusions

We investigated the preparation of WGCS and its membrane permeability. WGCS composed of 48.2% GCS, 20.6% CS, and 31.2% chitin units was prepared by the guanidinylation of a low-molecular-weight CS lactate with AP. The water solubility of WGCS was confirmed by DLS and transmittance analyses. In addition, we reveal that the higher chitin content in WGCS than in a common CS (<20%) is an important factor in achieving water solubility. Although WGCS showed higher toxicity toward HeLa cells in the MTT assay than CS lactate, WGCS also showed high viability (ca. 90%) at 0.25 mg/mL, comparable to that of CS lactate. The cellular internalization behaviors of R-WGCS and R-CS containing a fluorescent probe (rhodamine B), were compared by CLSM analysis and the fluorescence spectra of detached cells. Although both R-WGCS and R-CS were internalized into HeLa cells by incubation in transport medium (pH 7.4) containing R-WGCS and R-CS, the amount of WGCS molecules was ca. 2.5-fold higher than that of R-CS. In addition, colocalization of R-WGCS and LysoTracker Green supported the internalization of R-WGCS via endocytic pathways, and consequently, most of them accumulated in lysosomes. In addition, R-WGCS enhanced the internalization of F-BSA, which is used as a model protein. The internalized amount of F-BSA in the presence of R-WGCS was ca. 2-fold higher than that in the presence of R-CS. We attributed the higher enhancement to the strong electrostatic interaction between WGCS molecules and F-BSA at biological pH caused by the guanidino groups. Indeed, the affinity of the binding sites of WGCS was more than 10-fold higher than that of CS. We expect

novel formulation designs using WGCS and WGCS derivatives, such as complex formations with liposomes, inorganic materials, and/or polymers, to provide effective protein delivery systems. WGCS and WGCS derivatives would also provide novel DDSs for various types of drugs, such as genes, poorly soluble drugs, and poorly absorbable drugs. Therefore, this study is a first step toward the development of various DDSs based on WGCS and WGCS derivatives.

Acknowledgements The authors thank Prof. Hiroyuki Saimoto (Tottori University) for valuable discussions. This work was supported in part by JSPS KAKENHI Grant Number 19K05616.

Compliance with ethical standards

Conflict of interest The authors declare no competing interests.

References

1. Ninomiya K, Okura M. Nationwide comprehensive epidemiological study of rare diseases in Japan using a health insurance claims database. Orphanet J Rare Dis. 2022;17:140 https://doi.org/10.1186/s13023-022-02290-0.
2. Lipinski CA, Lombardo F, Dominy BW, Feeney PJ. Experimental and computational approaches to estimate solubility and permeability in drug discovery and development settings. Adv Drug Deliv Rev. 2001;46:3–26. https://doi.org/10.1016/s0169-409x(00)00129-0.
3. Amidi M, Mastrobattista E, Jiskoot W, Hennink WE. Chitosan-based delivery systems for protein therapeutics and antigens. Adv Drug Deliv Rev. 2010;62:59–82. https://doi.org/10.1016/j.addr.2009.11.009.
4. Bekale L, Agudelo D, Tajmir-Riahi HA. Effect of polymer molecular weight on chitosan-protein interaction. Colloids Surf B. 2015;125:309–17. https://doi.org/10.1016/j.colsurfb.2014.11.037.
5. Bizeau J, Mertz D. Design and applications of protein delivery systems in nanomedicine and tissue engineering. Adv Colloid Interface Sci. 2021;287:102334. https://doi.org/10.1016/j.cis.2020.102334.
6. Horn JM, Obermeyer AC. Genetic and covalent protein modification strategies to facilitate intracellular delivery. Biomacromolecules. 2021;22:4883–904. https://doi.org/10.1021/acs.biomac.1c00745.
7. Verma S, Goand UK, Husain A, Katekar RA, Garg R, Gayen JR. Challenges of peptide and protein drug delivery by oral route: current strategies to improve the bioavailability. Drug Dev Res. 2021;82:927–44. https://doi.org/10.1002/ddr.21832.
8. Zhang R, Nie T, Fang Y, Huang H, Wu J. Poly(disulfide)s: from synthesis to drug delivery. Biomacromolecules. 2022;23:1–19. https://doi.org/10.1021/acs.biomac.1c01210.
9. Izawa H, Haraya YT, Kawakami K. Cyclodextrin-grafted chitosans for pharmaceutical applications. Trends Glycosci Glycotechnol. 2017;29:E93–8.
10. Kumar MN, Muzzarelli RA, Muzzarelli C, Sashiwa H, Domb AJ. Chitosan chemistry and pharmaceutical perspectives. Chem Rev. 2004;104:6017–84. https://doi.org/10.1021/cr030441b.
11. Izawa H. Preparation of biobased wrinkled surfaces via lignification-mimetic reactions and drying: a new approach for developing surface wrinkling. Polym J. 2017;49:759–65. https://doi.org/10.1038/pj.2017.52.
12. Li B, Wang J, Moustafa ME, Yang H. Ecofriendly method to dissolve chitosan in plain water. ACS Biomater Sci Eng. 2019;5:6355–60. https://doi.org/10.1021/acsbiomaterials.9b00695.
13. Aranaz I, Alcantara AR, Civera MC, Arias C, Elorza B, Heras CA, et al. Chitosan: an overview of its properties and applications. Polymers. 2021;13. https://doi.org/10.3390/polym13193256.
14. Lee M, Nah JW, Kwon Y, Koh JJ, Ko KS, Kim SW, et al. Water-soluble and low molecular weight chitosan-based plasmid DNA delivery. Pharm Res. 2001;18:427–31. https://doi.org/10.1023/a:1011037807261.
15. Nakamichi A, Kadokawa J. Fabrication of Chitosan-based network polysaccharide nanogels. Molecules. 2022;27:8384.
16. Kubota N, Eguchi Y. Facile preparation of water-soluble N-acetylated chitosan and molecular weight dependence of its water-solubility. Polym J. 1997;29:123–7. https://doi.org/10.1295/polymj.29.123.
17. Suzuki S, Shimahashi K, Takahara J, Sunako M, Takaha T, Ogawa K, et al. Effect of addition of water-soluble chitin on amylose film. Biomacromolecules. 2005;6:3238–42. https://doi.org/10.1021/bm050486h.
18. Cho YW, Jang J, Park CR, Ko SW. Preparation and solubility in acid and water of partially deacetylated chitins. Biomacromolecules. 2000;1:609–14. https://doi.org/10.1021/bm000036j.
19. Gorochovceva N, Makuška R. Synthesis and study of water-soluble chitosan-O-poly(ethylene glycol) graft copolymers. Eur Polym J. 2004;40:685–91. https://doi.org/10.1016/j.eurpolymj.2003.12.005.
20. Mao S, Shuai X, Unger F, Wittmar M, Xie X, Kissel T. Synthesis, characterization and cytotoxicity of poly(ethylene glycol)-graft-trimethyl chitosan block copolymers. Biomaterials. 2005;26:6343–56. https://doi.org/10.1016/j.biomaterials.2005.03.036.
21. Kumar S, Dutta J, Dutta PK, Koh J. A systematic study on chitosan-liposome based systems for biomedical applications. Int J Biol Macromol. 2020;160:470–81. https://doi.org/10.1016/j.ijbiomac.2020.05.192.
22. Lombardo R, Musumeci T, Carbone C, Pignatello R. Nanotechnologies for intranasal drug delivery: an update of literature. Pharm Dev Technol. 2021;26:824–45. https://doi.org/10.1080/10837450.2021.1950186.
23. George M, Abraham TE. Polyionic hydrocolloids for the intestinal delivery of protein drugs: alginate and chitosan-a review. J Control Release. 2006;114:1–14. https://doi.org/10.1016/j.jconrel.2006.04.017.
24. Izawa H, Kinai M, Ifuku S, Morimoto M, Saimoto H. Guanidinylated chitosan inspired by arginine-rich cell-penetrating peptides. Int J Biol Macromol. 2019;125:901–5.
25. Izawa, H, Kinai, M, Ifuku, S, Morimoto, M & Saimoto, H. Guanidinylation of chitooligosaccharides involving internal cyclization of the guanidino group on the reducing end and effect of guanidinylation on protein binding ability. Biomolecules. 2019;9. https://doi.org/10.3390/biom9070259.
26. Mogaki R, Hashim PK, Okuro K, Aida T. Guanidinium-based "molecular glues" for modulation of biomolecular functions. Chem Soc Rev. 2017;46:6480–91. https://doi.org/10.1039/c7cs00647k.
27. Khafagy ES, Morishita M. Oral biodrug delivery using cell-penetrating peptide. Adv Drug Deliv Rev. 2012;64:531–9.
28. Kristensen M, Nielsen HM. Cell-penetrating peptides as carriers for oral delivery of biopharmaceuticals. Basic Clin Pharm Toxicol. 2016;118:99–106. https://doi.org/10.1111/bcpt.12515.
29. Murayama T, Masuda T, Afonin S, Kawano K, Takatani-Nakase T, Ida H, et al. Loosening of lipid packing promotes oligoarginine entry into cells. Angew Chem Int Ed. 2017;56:7644–7. https://doi.org/10.1002/anie.201703578.

30. Takeuchi T, Futaki S. Current understanding of direct translocation of arginine-rich cell-penetrating peptides and its internalization mechanisms. Chem Pharm Bull. 2016;64:1431–7. https://doi.org/10.1248/cpb.c16-00505.
31. Hu Y, Du YM, Yang JH, Kennedy JF, Wang XH, Wang LS. Synthesis, characterization and antibacterial activity of guanidinylated chitosan. Carbohydr Polym. 2007;67:66–72. https://doi.org/10.1016/j.carbpol.2006.04.015.
32. Sahariah P, Oskarsson BM, Hjalmarsdottir MA, Masson M. Synthesis of guanidinylated chitosan with the aid of multiple protecting groups and investigation of antibacterial activity. Carbohydr Polym. 2015;127:407–17. https://doi.org/10.1016/j.carbpol.2015.03.061.
33. Salama A, Hasanin M, Hesemann P. Synthesis and antimicrobial properties of new chitosan derivatives containing guanidinium groups. Carbohydr Polym. 2020;241:116363. https://doi.org/10.1016/j.carbpol.2020.116363.
34. Zhang X, Fan J, Lee C, Kim S, Chen C, Lee M. Supramolecular hydrogels based on nanoclay and guanidine-rich chitosan: injectable and moldable osteoinductive carriers. ACS Appl Mater Interfaces. 2020;12:16088–96. https://doi.org/10.1021/acsami.0c01241.
35. Yano K, Masaoka Y, Kataoka M, Sakuma S, Yamashita S. Mechanisms of membrane transport of poorly soluble drugs: role of micelles in oral absorption processes. J Pharm Sci. 2010;99:1336–45. https://doi.org/10.1002/jps.21919.
36. Shi H, He X, Yuan Y, Wang K, Liu D. Nanoparticle-based biocompatible and long-life marker for lysosome labeling and tracking. Anal Chem. 2010;82:2213–20. https://doi.org/10.1021/ac902417s.
37. Kamei N, Shigei C, Hasegawa R, Takeda-Morishita M. Exploration of the key factors for optimizing the in vivo oral delivery of insulin by using a noncovalent strategy with cell-penetrating peptides. Biol Pharm Bull. 2018;41:239–46.
38. Uusna J, Langel K, Langel U. Toxicity, immunogenicity, uptake, and kinetics methods for CPPs. Methods Mol Biol. 2015;1324:133–48. https://doi.org/10.1007/978-1-4939-2806-4_9.
39. Cavanagh RJ, Smith PA, Stolnik S. Exposure to a nonionic surfactant induces a response akin to heat-shock apoptosis in intestinal epithelial cells: implications for excipients safety. Mol Pharm. 2019;16:618–31. https://doi.org/10.1021/acs.molpharmaceut.8b00934.
40. Muller-Esparza H, Osorio-Valeriano M, Steube N, Thanbichler M, Randau L. Bio-layer interferometry analysis of the target binding activity of CRISPR-cas effector complexes. Front Mol Biosci. 2020;7:98. https://doi.org/10.3389/fmolb.2020.00098.
41. Fivash M, Towler EM, Fisher RJ. BIAcore for macromolecular interaction. Curr Opin Biotechnol. 1998;9:97–101. https://doi.org/10.1016/s0958-1669(98)80091-8.
42. Du JR, Su X, Feng X. Chitosan/sericin blend membranes for adsorption of bovine serum albumin. Can J Chem Eng. 2017;95:954–60. https://doi.org/10.1002/cjce.22760.